JOM
DOI: 10.1007/s11837-017-2579-0
© 2017 The Minerals, Metals & Materials Society

Direct Observation Through In Situ Transmission Electron Microscope of Early States of Crystallization in Nanoscale Metallic Glasses

Y. XIE,[1,2,3] S. SOHN,[1,3] J. SCHROERS,[1,3] and J.J. CHA[1,2,3,4]

1.—Department of Mechanical Engineering and Materials Science, Yale University, New Haven, CT 06511, USA. 2.—Energy Sciences Institute, Yale West Campus, West Haven, CT 06516, USA. 3.—Center for Research on Interface Structures and Phenomena, Yale University, New Haven, CT 06511, USA. 4.—e-mail: judy.cha@yale.edu

Crystallization is a complex process that involves multiscale physics such as diffusion of atomic species over multiple length scales, thermodynamic energy considerations, and multiple possible intermediate states. In situ crystallization experiments inside a transmission electron microscope (TEM) using nanostructured metallic glasses (MGs) provide a unique platform to study directly crystallization kinetics and pathways. Here, we study the embryonic state of eutectic growth using Pt-Ni-Cu-P MG nanorods under in situ TEM. We directly observe the nucleation and growth of a Ni-rich polymorphic phase, followed by the nucleation and slower growth of a Cu-rich phase. The suppressed growth kinetics of the Cu-rich phase is attributed to locally changing chemical compositions. In addition, we show that growth can be controlled by incorporation of an entire nucleus instead of individual atoms. Such a nucleus has to align with the crystallographic orientation of a larger grain before it can be incorporated into the crystal. By directly observing the crystallization processes, particularly the early stages of non-polymorphic growth, in situ TEM crystallization studies of MG nanostructures provide a wealth of information, some of which can be applied to typical bulk crystallization.

Understanding crystallization is important to control microstructures of materials. As demonstrated in crystallization studies of many different material systems,[1–3] it is now generally realized that classic understanding of crystallization is not sufficient to capture the general complexity of crystallization processes.[4–7] Challenges have been partly the lack of direct in situ tools that allow us to track the morphological as well as compositional changes of the system during crystallization with sufficient time and spatial resolution.

In recent years, major advances in in situ TEM techniques have occurred, which enable direct study of crystallization. These advances include aberration correctors that allow subatomic resolution,[8–10] modern in situ thermal holders with precise temperature control and excellent thermal stability,[11] and fast charge-coupled device (CCD) read-out for acquiring movies with high temporal resolution.[12] As a result of these advances, several seminal works on crystallization have been conducted to show that intermediated states, subcritical nuclei, and possible medium range order play an important role during crystal growth.[13–15] In addition to technological developments in in situ TEM, sample preparation methods compatible with TEM imaging have been promoted and provide a new route to investigate the complex crystallization processes.[16,17]

Metallic glasses (MGs), in particular bulk metallic glasses (BMGs), are a good model system for studying glass physics, such as understanding of glass forming ability, as a result of their simple metallic bonds, large supercooled liquid region, and slow crystallization kinetics.[18,19] They also hold promise for mechanical and biological applications because of their mechanical strength and elasticity, corrosion-resistance, and bio-compatibility.[20–22] In the present work, we exploit a previously developed thermoplastic forming technique to synthesize MGs nanorods with varying diameters and apply in situ

Published online: 19 September 2017

heating inside a TEM to visualize the crystallization process. We directly observe two crystallization phenomena, which highlight the complexity of the crystallization process in multicomponent MG nanorod systems.

MGs nanorods were made by thermoplastic-based nanomolding (Fig. 1).[23] By pressing a heated MG plate into a mold where the processing temperatures are in the supercooled liquid region between the glass transition temperature and the crystallization temperature, the MG was thermoplastically formed into nanorods while retaining its amorphous structure. The synthesis of $Pt_{57.5}Cu_{14.7}Ni_{5.3}P_{22.5}$ MGs nanorods used in this study begins with alloying of high-purity constituents with nominal compositions by induction melting. The synthesized bulk MG is then heated to 260°C and placed on porous anodized aluminum oxide (AAO from Synkera Inc.) mold (Fig. 1a and b). Nanorods were thermoplastically formed by pressing the heated bulk MG into the AAO mold (Fig. 1c). To release the nanorods, we dissolve the AAO mold in a 20% potassium hydroxide (KOH) solution at 80°C (Fig. 1d). With sonication, nanorods break off and are collected in isopropyl alcohol (IPA) (Fig. 1e). The size of nanorods is mainly determined by the pore size of the AAO mold and can range from 10 nm to 200 nm in diameter.

First we show an example of using in situ TEM to observe a crystallization process in a 45-nm MG nanorod (Fig. 2). The nanorod was wet-transferred onto an in situ thermal chip, which can be heated up to 1100°C. The nanorod was heated to and held at 380°C for the entire in situ experiment. During this time, structure changes were recorded in a dark-field (DF) imaging mode. Detailed analysis of the chemical composition and the crystal structure was carried out using energy dispersive x-ray spectroscopy (EDX) and high-resolution TEM imaging (HRTEM) after the heating experiment. In Fig. 2 and supplementary video 1, we observe two crystalline phases with different crystallization kinetics, chemical compositions, and crystal structures. In Fig. 2a, a Ni-rich phase (denoted with an arrow in the left-most image) first appears, which grows at the growth rate of 72 ± 0.5 nm/s. This is followed by an emergence of a Cu-rich phase (at t = 14 s), which grows much slower at the growth rate of 18 ± 0.2 nm/s. The Cu-rich phase eventually stops growing even though the rod is still at 380°C. We attribute the slow growth of the Cu-rich phase to the unfavorable chemical composition in the glass region. The chemical information was obtained by EDX after the heating experiment was finished. Figure 2b shows EDX mapping of Ni and Cu, which

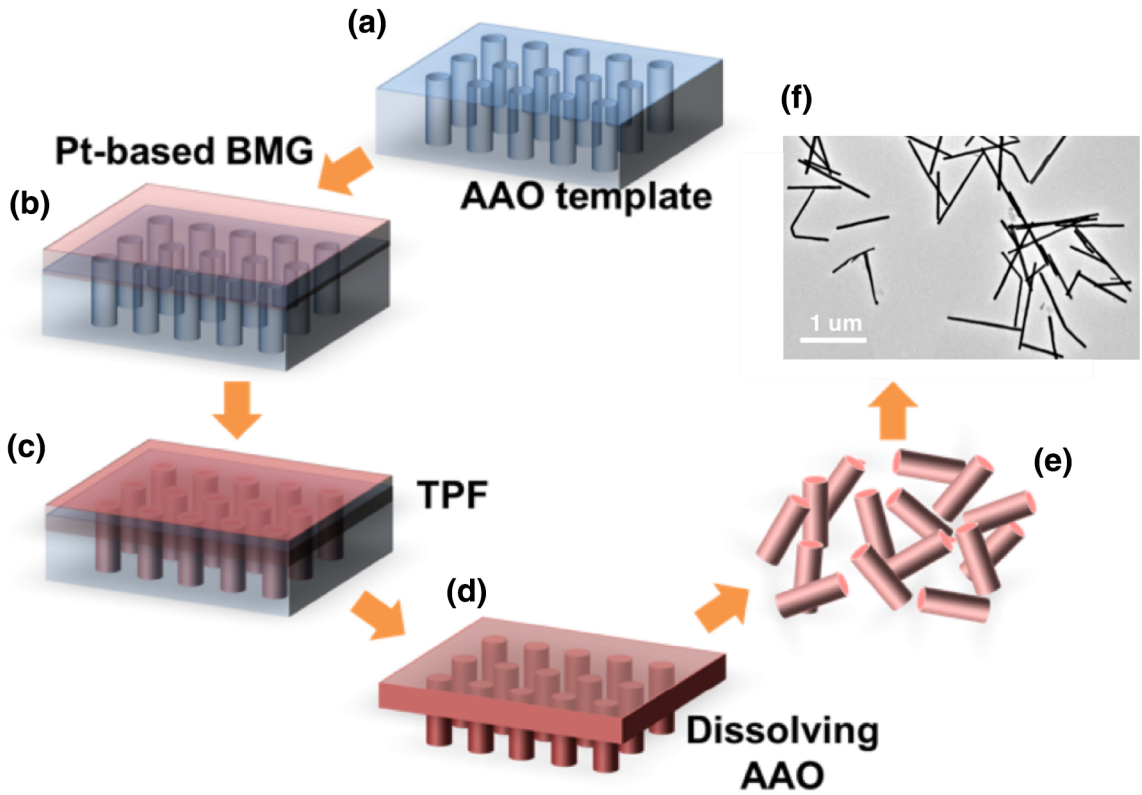

Fig. 1. Schematic of synthesis of MGs nanorods. (a) A commercial anodized aluminum oxide (AAO) template with a porous pattern. (b) A piece of bulk MG is heated up and placed between the AAO template and a custom-built heating plate (heating plate not shown). (c) The MG plate is pressed down onto the AAO mold to thermoplastically form nanorods. (d) The AAO template is dissolved in a 20 wt.% potassium hydroxide (KOH) solution. (e) MG nanorods are released by sonication. (f) A TEM image of nanorods. (a–e) adapted from Ref. [1].

shows a Ni-rich region and a Cu-rich region, corresponding to the two grains observed in the DF in situ TEM movie (supplementary video 1).

These two phases not only have different chemical compositions but also different crystal structures, which were studied by fast Fourier transformation (FFT) of the selected regions from the HRTEM image, as shown in Fig. 2c. The diffractograms of the Ni-rich and Cu-rich regions show distinct diffraction spots. The Ni-rich region shows six diffraction spots, while the Cu-rich region shows two diffraction spots. We cannot eliminate the possibility that the different diffractograms are a result of tilting of the crystalline grains. From previous bulk studies, four phases are reported for the Pt-based metallic glass: platinum phosphide (P_2Pt_5) with monoclinic C2/c structure, copper phosphide (CuP_2) with P21/c structure, NiP_2, and NiPt.[24] Thus, the Cu-rich phase may adapt the P21/c structure. The EDX spectrum of the Cu-rich region shows no Ni (Fig. 2d). For the Ni-rich phase, the EDX spectrum (Fig. 2d) shows the presence of Cu, suggesting that it may be a metastable phase. We note that the Ni/Cu ratio of the Ni-rich phase is higher than that of the glass. As a result of the limited diffraction information, however, further experiments are needed to identify the crystal structure.

Another crystallization phenomenon we observe via in situ TEM crystallization study is shown in Fig. 3. A 45-nm MG nanorod was again heated to and held at 380°C. With this example, we capture a scenario in which a small crystallite affects the growth of a large grain during the isothermal crystallization process. Figure 3a shows snapshots from a dark field TEM movie (supplementary video 2), which records the merging process of a small crystallite and a growing grain. The small crystallite is denoted by the white arrow in Fig. 3a. At the 3-s mark (left most snapshot), a large grain is observed, which grows from the bottom to the top direction. At the 6-s mark, the growth front of the large grain touches the small crystallite, at which point the growth rate of the large grain decreases significantly. The small crystallite gets pushed up by the growing grain. The crystallite also rotates around, which is evident by the intensity changes in the DF TEM. For example, the intensity contrasts at the time stamp of 41 s and 48 s are different for the small crystallite. At the 53-s mark, the small

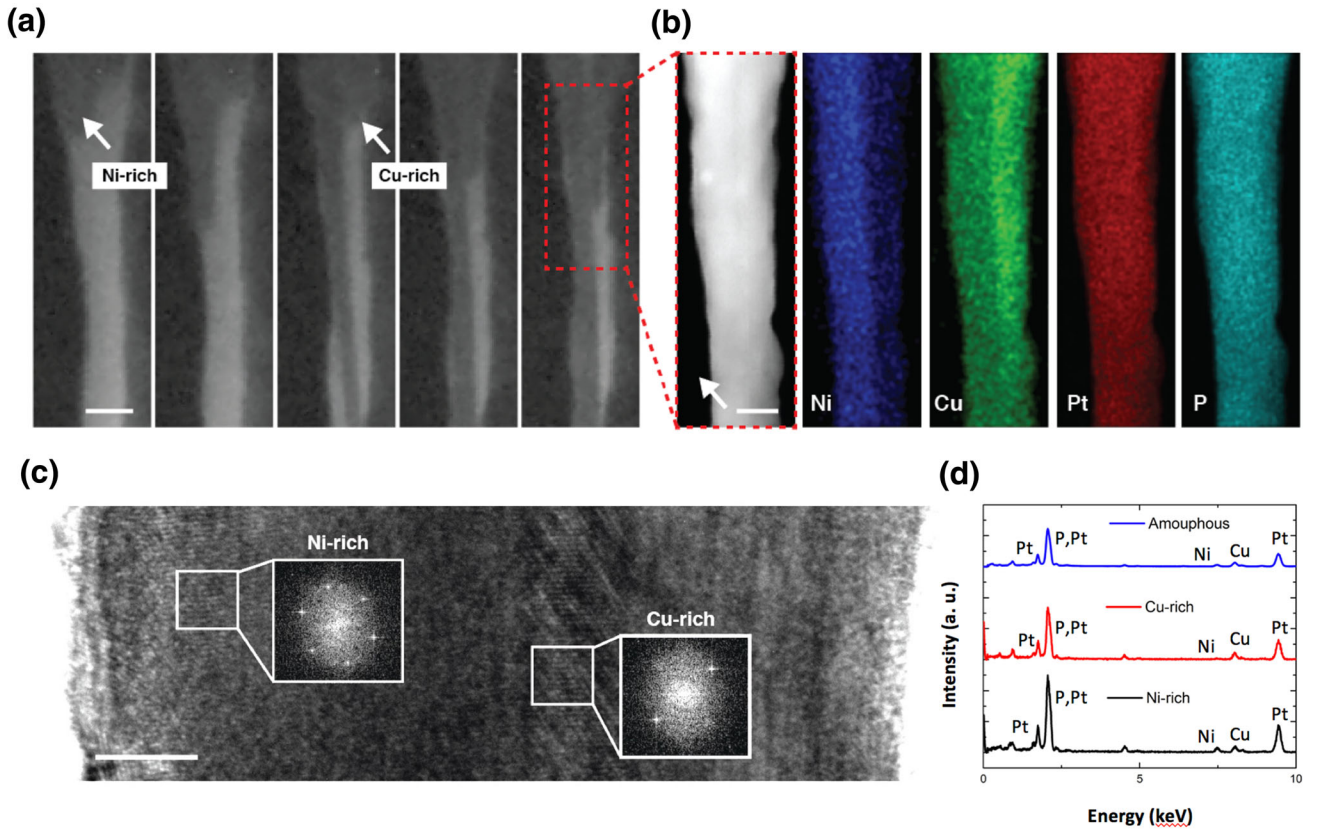

Fig. 2. Crystallization of a 45-nm nanorod isothermally heated at 380°C. (a) Snapshots from a DF TEM movie that shows growth of a Ni-rich phase and a Cu-rich phase with different growth rates. Two grains are indicated by the dashed lines. (b) Energy-dispersive x-ray mapping of Ni and Cu on the crystallized nanorod. (c) A high-resolution TEM image with selected area fast Fourier transformation patterns showing possibly different crystal structures. Scale bar is 30 nm in (a) and (b) and 6 nm in (c). (d) EDX spectrum of the glass (blue), the Cu-rich phase (red), and the Ni-rich phase (black) (Color figure online).

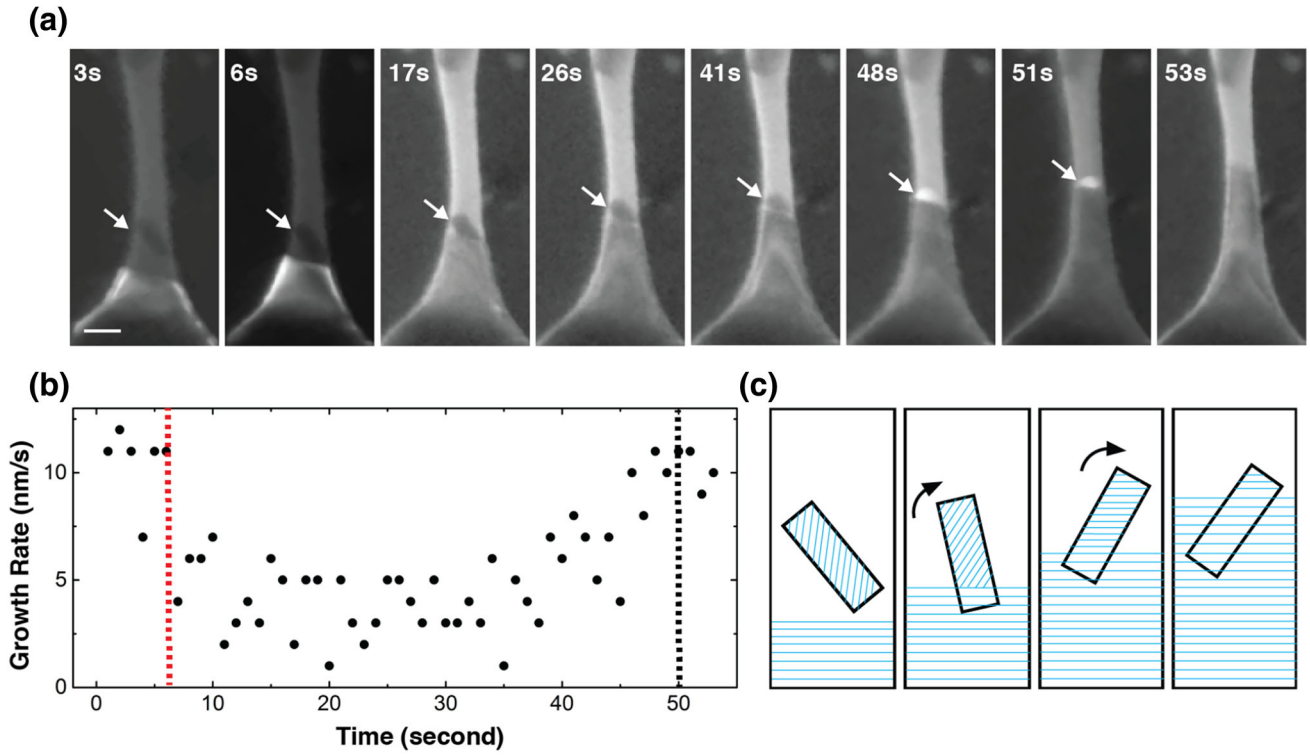

Fig. 3. Small crystallite merged into a large crystal grain. A MG nanorod is isothermally heated at 380°C. (a) A small crystallite (white arrow) impinges the growth front of the large grain. The crystallite eventually disappears. (b) A plot of the measured growth rates during the crystallization shows suppression of the large grain growth during the merging event. The red dotted line marks the time at which the small crystallite meets the growing grain, and the black dotted line marks the time at which the small crystallite is fully incorporated by the growing grain. (c) A schematic diagram shows how a small crystallite with a different crystal orientation or structure rotates and merges into the larger grain. Scale bar in (a) = 35 nm (Color figure online).

crystallite begins to get incorporated by the large grain. Figure 3b plots the measured growth rate changes during this experiment. When the large grain meets the small crystallite, the growth is impinged as shown by the suppressed growth rate. Once the small crystallite is fully incorporated into the large grain, the growth rate resumes its original value. Similar observations have been reported in other material systems.[25–28] We note that crystallization occurs from the bottom of the nanowire where the rod is wider. We attribute this to the likelihood that more nuclei are present in a wider region of the rod, which is in agreement with our previous study.[1]

We assume the suppression of the large grain growth is from the crystal orientation difference between the small crystallite and the large grain, which is depicted in the Fig. 3c schematic. As a result of the experimental limitations of in situ experiments, chemical information and electron diffraction information could not be obtained during the crystallization event. Thus, we cannot rule out potential chemical composition differences or crystal structure differences. The slowdown of the large grain propagation occurs when it approaches the crystallite but before the actual collision, which suggests a possible strong interaction between the two. Because of the possibility that the two grains might be chemically different, the slowed growth of the large grain before the collision could indicate chemical fields that have steep compositional gradients. In Fig. 3a, we also observe that the morphology of the small crystallite gradually changes, indicating atomic diffusions from the small crystallite to the large grain. Thus, atomic diffusions as well as compositional gradients, in addition to the crystal orientation mismatch, could explain the slowdown of the crystallization of the large grain.

In situ TEM crystallization experiments provide direct visualization of complex crystallization processes. The nanometer resolution easily achievable in a TEM enables close investigation of crystallization events in real time. Even though some of observed crystallization processes might be a result of size confinement, other aspects that are discussed here might be representative for bulk crystallization as well.

ELECTRONIC SUPPLEMENTARY MATERIAL

The online version of this article (doi:10.1007/s11837-017-2579-0) contains supplementary material, which is available to authorized users.

REFERENCES

1. S. Sohn, Y. Jung, Y. Xie, C. Osuji, J. Schroers, and J.J. Cha, *Nat. Commun.* 6, 8157 (2015).
2. D. Jacobsson, F. Panciera, J. Tersoff, M.C. Reuter, S. Lehmann, S. Hofmann, K.A. Dick, and F.M. Ross, *Nature* 531, 317 (2016).
3. J. Baumgartner, A. Dey, P.H. Bomans, C. Le Coadou, P. Fratzl, N.A. Sommerdijk, and D. Faivre, *Nat. Mater.* 12, 310 (2013).
4. Y.U. Gong, C.E. Killian, I.C. Olson, N.P. Appathurai, A.L. Amasino, M.C. Martin, L.J. Holt, F.H. Wilt, and P. Gilbert, *Proc. Natl. Acad. Sci. U.S.A.* 109, 6088 (2012).
5. R.L. Penn and J.F. Banfield, *Science* 281, 969 (1998).
6. W.J. Habraken, J. Tao, L.J. Brylka, H. Friedrich, L. Bertinetti, A.S. Schenk, A. Verch, V. Dmitrovic, P.H. Bomans, and P.M. Frederik, *Nat. Commun.* 4, 1507 (2013).
7. K.-S. Cho, D.V. Talapin, W. Gaschler, and C.B. Murray, *J. Am. Chem. Soc.* 127, 7140 (2005).
8. C. Chen, Y. Kang, Z. Huo, Z. Zhu, W. Huang, H.L. Xin, J.D. Snyder, D. Li, J.A. Herron, and M. Mavrikakis, *Science* 343, 1339 (2014).
9. B.L. Mehdi, M. Gu, L.R. Parent, W. Xu, E.N. Nasybulin, X. Chen, R.R. Unocic, P. Xu, D.A. Welch, and P. Abellan, *Microsc. Microanal.* 20, 484 (2014).
10. M.A. van Huis, N.P. Young, G. Pandraud, J.F. Creemer, D. Vanmaekelbergh, A.I. Kirkland, and H.W. Zandbergen, *Adv. Mater.* 21, 4992 (2009).
11. E. Lewis, T. Slater, E. Prestat, A. Macedo, P. O'Brien, P. Camargo, and S. Haigh, *Nanoscale* 6, 13598 (2014).
12. Z. Wang, S. Joshi, S.E. Savel'ev, H. Jiang, R. Midya, P. Lin, M. Hu, N. Ge, J.P. Strachan, and Z. Li, *Nat. Mater.* 16, 101 (2017).
13. J. De Yoreo, *Nat. Mater.* 12, 284 (2013).
14. J.J. De Yoreo, P.U. Gilbert, N.A. Sommerdijk, R.L. Penn, S. Whitelam, D. Joester, H. Zhang, J.D. Rimer, A. Navrotsky, and J.F. Banfield, *Science* 349, aaa6760 (2015).
15. A. Dey, P.H. Bomans, F.A. Müller, J. Will, P.M. Frederik, G. de With, and N.A. Sommerdijk, *Nat. Mater.* 9, 1010 (2010).
16. U. Anand, J. Lu, D. Loh, Z. Aabdin, and U. Mirsaidov, *Nano Lett.* 16, 786 (2016).
17. L. Fei, S.M. Ng, W. Lu, M. Xu, L. Shu, W.-B. Zhang, Z. Yong, T. Sun, C.H. Lam, and C.W. Leung, *Nano Lett.* 16, 7875 (2016).
18. R. Busch, J. Schroers, and W. Wang, *MRS Bull.* 32, 620 (2007).
19. R. Busch, *JOM* 52, 39 (2000).
20. C.A. Schuh, T.C. Hufnagel, and U. Ramamurty, *Acta Mater.* 55, 4067 (2007).
21. D. Curry and J. Knott, *Met. Sci.* 10, 1 (1976).
22. G. Kumar, A. Desai, and J. Schroers, *Adv. Mater.* 23, 461 (2011).
23. G. Kumar, H.X. Tang, and J. Schroers, *Nature* 457, 868 (2009).
24. B.A. Legg, J. Schroers, and R. Busch, *Acta Mater.* 55, 1109 (2007).
25. M.A. van Huis, L.T. Kunneman, K. Overgaag, Q. Xu, G. Pandraud, H.W. Zandbergen, and D. Vanmaekelbergh, *Nano Lett.* 8, 3959 (2008).
26. J.F. Banfield, S.A. Welch, H. Zhang, T.T. Ebert, and R.L. Penn, *Science* 289, 751 (2000).
27. J. Lee, J. Yang, S.G. Kwon, and T. Hyeon, *Nat. Rev. Mater.* 1, 16034 (2016).
28. J.M. Yuk, J. Park, P. Ercius, K. Kim, D.J. Hellebusch, M.F. Crommie, J.Y. Lee, A. Zettl, and A.P. Alivisatos, *Science* 336, 61 (2012).